Measurement: Sensors 29 (2023) 100880

Contents lists available at ScienceDirect

Measurement: Sensors

journal homepage: www.sciencedirect.com/journal/measurement-sensors

An adaptive optimum weighted mean filter and bilateral filter for noise removal in cardiac MRI images

R. Radhika *, Rashima Mahajan

Computer Science and Engineering, Manav Rachna International Institute of Research and Studies, Faridabad, India

ARTICLE INFO

Keywords:
MRI image
Noise suppression
Filtering
Adaptive optimum weighted mean filter
Bilateral filter
Impulsive noise and crow optimization algorithm

ABSTRACT

Medical diagnosis greatly benefits from the use of MRI images. There have been many MRI image enhancement algorithms proposed over the years to aid doctors in disease diagnosis. Conventional image enhancing methods, nevertheless, may also boost the noise that was already there in the captured picture, which might cause distortion, which is unfavourable for the disease diagnosis. Therefore, an appropriate technique for noise suppression is necessary. An attempt has been made to incorporate a two-step filtering based algorithm for noise removal in cardiac MRI images while maintaining the images crucial compositional elements, such as their borders and textures. A combination of adaptive optimum weighted mean filter (AOWMF) and bilateral filter (BF) has been implemented to reduce impulsive noise and Gaussian noise that are both present as mixed noise. The fundamental idea of the AOWMF approach includes the detection of noise pixels using Crow Optimization Algorithm (COA), and replacing them with an optimum weighted mean value depending on a criterion of maximization fitness function. Peak Signal to Noise Ratio (PSNR) and Structural Similarity Index Measure (SSIM) have been used to assess the effectiveness of the employed noise reduction technique. The result analysis are experimented in MATLB which reveals that proposed method is able to achieve high PSNR and SSIM and further, this method has the potential to enhance more detail structures of the input cardiac MRI images than existing methods.

1. Introduction

Magnetic resonance imaging (MRI) is a strong technique for the imaging of the heart structure and function in order to diagnose a number of cardiac disorders. In an effort to improve the contrast between the myocardial and the backdrop, a method was recently devised to capture cine heartbeats that result in the blood signal being completely black (null). Nevertheless, the method has a high noise level that restricts the contrast-to-noise ratio by being an inherent problem [1, 2]. Image registration, segmentation, classification, and visualization are impeded by excessive noise levels. Before doing any additional image processing, MRI noise removal is necessary carried out in order to achieve trustworthy image analysis findings. The most crucial stage of image pre-processing is hence image denoising. Denoising remains difficult despite the existence of several ways for doing so since they often result in artifacts and unclear images [3].

Low signal to noise ratio (SNR) devices are sometimes used to record medical images. The tissue characterisation on such images fails and it is challenging to distinguish anatomical features because of the low SNR. In order to do any additional processing or analysis, denoising of the MRI images is thus a necessary procedure. The literature has described the Rician distribution of noise in MR images. Hence, it is impossible to eliminate these disturbances using ordinary filters [4]. The object borders and fine features are degraded by the linear spatial filtering approach. The current research demonstrated the capability of wavelet-based approaches, such as wavelet thresholding, to remove the noise coefficient. By comparing the calculated noisy wavelet coefficient with other wavelet coefficients, wavelet thresholding calculates the threshold value and removes the noisy pixel intensity value from high frequency content [5]. Also, to report these problems several de-noising methods, including the Weiner, Gaussian, and median filters, have been created.

The goal of noise reduction methods in MRI is to get slowly fluctuating or piecewise constant signals in homogeneous tissue regions while retaining tissue boundaries. In terms to user engagement, applicability to different MR collection techniques, noise reduction, boundary preservation, robustness, and all of these factors, and computational cost, no one approach has emerged as being better than the others. At this time,

* Corresponding author.
E-mail addresses: radhips8@gmail.com (R. Radhika), rashima.fet@mriu.edu.in (R. Mahajan).

https://doi.org/10.1016/j.measen.2023.100880
Received 6 April 2023; Received in revised form 2 August 2023; Accepted 13 August 2023
Available online 14 August 2023

with MRI imaging techniques and their varieties constantly evolving. With this motivation two filtering methods have been implemented for denoising of input cardiac MRI images in the proposed work.

In this research, an effort is made to eliminate background noise in the cardiac signal input MRI images using adaptive optimum weighted mean filter (AOWMF) and bilateral filter (BF). Most often heard in medical MRI scans are the noises known as "salt and pepper," "speckle," "rician," "gaussian," and "poison noise". The performance of these noise removing filters has been examined for various types of noise including Gaussian, gaussian-like, speckled, fuzzy, and poison noise. These techniques have been assessed using criteria such as the image file size, histogram, and clarity scale. According to the experimental findings, the BF filter performs better at reducing rician noise than the AOWMF filter does at removing speckle and gaussian noise for grayscale images.

The outline of this research paper includes the review of filters for MRI imaging in the first section. The details of proposed filters viz., AOWMF and BF are presented in the second section. In the third section, experimental findings and comparisons are provided, and the fourth section concludes and discusses the implications for the future.

2. Literature survey

Denoising magnetic resonance (MR) images improves registration, segmentation, and parameter estimation. A high-performance, nonlocal noise filter was described for MR image sets comprising progressively-weighted multispectral images [6]. This filter added spectrums to the nonlocal maximum likelihood filter (NLML). Using synthetic and in vivo T2 and T1-weighted brain imaging data, the effectiveness of the nonlocal-means (NLM), its multispectral variation (MS-NLM), and the nonlocal maximum likelihood (NLML) filters was evaluated. The visual inspection and quantitative research showed that all filters significantly decreased noise and multispectral information may improve filtering quality.

Another study used frequency domain filters to take advantage of the system matrix's unique structure and reduce noise [7]. Typically, a calibration measurement was used to collect the system matrix, it involved assessing system reaction at different field-of-view locations. It was shown that using the denoised system matrix during image reconstruction results in greater resolution and a higher signal-to-noise ratio. By averaging the intensities in a pixel's adaptive homogeneous neighbourhood, a revolutionary smoothing technique known as non-stationarity adaptive filtering was put into practice [8]. Maps of spatial-directional non-stationarity measure and five constraints were used to determine the latter. An anisotropic diffusion technique utilized in diffusion weighted (DW) picture smoothing was compared to the proposed approach. Even with noisy data, the suggested technique balances homogenous region smoothness and boundary preservation well. Hence, homogeneously consistent tensor fields and coherent fibres arise. Experimental findings using genuine and simulated human DW images showed.

In the literature, it was also investigated how to analyse medical images generally using a learned guiding map and a locally linear guided filter [9]. The output images were meant to only be processed by the guided filter, even though the guidance map might be trained to be task-optimal from beginning to finish. Performance was measured using picture super resolution and denoising. The results were analysed using multi-modal magnetic resonance imaging and cross-modal computed tomography datasets. The suggested method was comparable to state-of-the-art methods for both tasks. Moreover, it was shown that, unlike with traditional techniques, the content of the input image remained mostly unaffected after processing. The suggested pipeline also provided improved resilience against adversarial assaults and degraded input.

By introducing a hybrid multi-resolution filter to denoised MRI images affected by salt and pepper noise, wavelet transform was used to increase image resolution [10]. Three value-weighted filters plus a filter

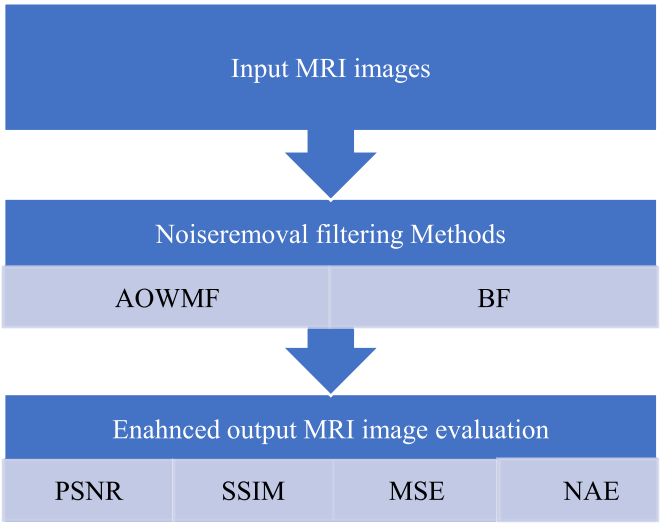

Fig. 1. General framework diagram optimum weighted mean filter and bilateral filter for noise removal.

based on similarity made up the hybrid filter. The three value weighted filter's noisy pixels were identified using a variable local window. The three-value technique was used to rebuild noisy pixels using the window's noise-free pixels. A variable local window recreates noisy pixels in the similarity-based filter. Based on the similarity between the noisy and noise-free pixel sequences, window was utilized to recreate the noisy pixel sequence. Last but not least, the reconstructed image's resolution was improved using the wavelet transform.

Images-based quantitative metrics are challenging to quantify because of rician noise. Anti-additive noise performance of the non-local means (NLM) filter has been shown. The properties of both Rician noise and the NLM filter were taken into consideration while creating a frame for a pre-smoothing NLM (PSNLM) filter and image modification [11]. An image that may be considered as additive noise is created from noisy MRI in the PSNLM frame. Second, a conventional denoising technique is used to pre-smooth the converted MRI. Third, weights from the pre-smoothed image are calculated and added to the modified MRI before the NLM filter is used. To acquire the denoising findings, inverse transformation is then used to the denoised MRI.

So in this work the proposed method utilized adaptive technique in WMF method to remove Speckle and Gaussian Noise from MRI images with Optimization Algorithm and then each part has been denoised by using bilateral filter to remove the Rician type of noises. However, in certain situations median filtering is better and two of its main advantages are: I) the proposed filtering preserves sharp edges, whereas linear low-pass filtering blurs such edges. II) the proposed filters are very efficient for smoothing of spiky noise.

3. Materials and methods

In order to get MR images with great spatial resolution, surface coils, particularly phased-arrays, are often utilized in MR machines. Because of the coil sensitivity profile, the signal intensities on images taken with these coils exhibit a non-uniform map. When quantitative information from the images is required, these smooth intensity variations despite having no effect on visual diagnosis become serious problems. The AMRG Cardiac MRI Atlas dataset has been used in this research work. The AOWMF has been utilized to pre-process the dataset imported in MATLAB workspace which is one of the widely used methods for denoising based on Weighted Median Filter (WMF). The proposed method utilized adaptive technique in WMF method to remove Speckle and Gaussian Noise from MRI images with Crow Optimization Algorithm (COA) and then each part has been denoised by using bilateral

filter to remove the Rician type of noises. The outline of the methodology is as depicted in Fig. 1. The performance of the implemented method has been analysed using the parameters viz., PSNR, structural similarity index measurement (SSIM), mean square error (MSE) and normalized absolute error (NAE).

3.1. Image acquisition of cardiac MRI dataset

Cardiac MRI image dataset has been imported into MATLAB workspace. Input cardiac MRI images from two online available databases SCMR consensus and AMRG Atlas have been analysed in this research work. The mixed-normal, myocardial infarction, and hypertrophy patients make up the SCMR consensus dataset [12]. The AMRG Heart MRI Atlas of a healthy patient's heart was captured using the Auckland MRI Research Group's Siemens Avanto scanner. College and high school students, MR technicians, clinicians, and patients may use the atlas to learn about heart anatomy and MRI, a critical and emerging cardiology method. Images from the Atlas have also been collected of the aortic arch and right ventricular outflow tract in addition to the conventional imaging planes of axial, coronal, and sagital. Each individual subject's tagged MRI images of a normal heart make up the AMRG Heart MRI Atlas. This is an educational resource aimed at those wishing to learn about the heart's anatomy as well developing experience with cardiac MRI.

3.2. Filtering process for noise removal

Getting rid of the noise will help to get the image ready for analysing in further stages, noise reduction in MRI image pre-processing is a crucial step. Nevertheless, various kinds of noise have varying degrees of influence on the clarity of the image, this often reduces the accuracy of computer-aided diagnostic instruments and human interpretation.

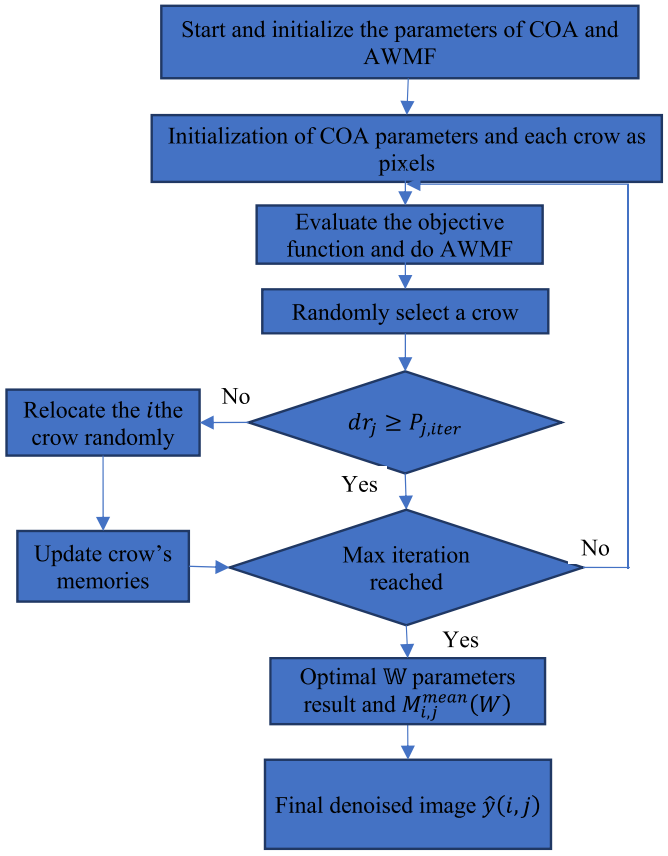

Fig. 2. The flow diagram of AOWMF methodology for noise elimination.

Another problem is choosing filtering techniques based on noise model and filter reconstruction ability to reduce noise and maintain high quality images. To eliminate the additive noise present in the input cardiac MRI images, i.e., Gaussian, Salt and Pepper, and Speckle Noise, two filtering methods, such as AOWMF and BF, have been developed in this study. The AOWMF has been utilized to denoise the noisy images during pre-processing. BF is used to improve the de-noised images that is obtained.

3.2.1. Adaptive weighted mean filter (AWMF)

As compared to conventional mean filter, which employs a fixed window size to remove low levels of salt and pepper noise, adaptive weighted mean filter utilizes variable window size to reduce high levels of noise that significantly lower the quality of MR images. The window size is periodically increased in the adaptive weighted mean filter until two subsequent windows' highest and lowest pixel values coincide. If the window's center pixel value is either the lowest or highest, it will be restored to the average weighted value. If the center pixel value is neither the lowest or maximum, the intensity value stays the same. $x_{i,j}$ for the original image of size denotes the coordinate system's center pixel intensity value $M \times N\ (x,y)$. The dynamic range (DR) is given by $DR_{min} \leq x_{i,j} \leq DR_{max}$ The representation of a corrupted image is dr. The minimum and maximum dynamic ranges, DR_{min} and DR_{max} are used to replace an image's faulty pixel utilizing equation (1):

$$\mathrm{dr}_{\mathrm{i,j}} = \begin{cases} \mathrm{DR}_{\min} & \text{with } \mathbb{P}\ \mathrm{a} \\ \mathrm{DR}_{\max} & \text{with } \mathbb{P}\ \mathrm{b} \\ \mathrm{x}_{\mathrm{i,j}} & \text{with } \mathbb{P}\ 1-\mathrm{a}-\mathrm{b} \end{cases} \tag{1}$$

Where: $noise = a + b$, $\boldsymbol{a}$ and $\boldsymbol{b}$ are denoted as the probabilities $\mathbb{P}$ maximum (speckle) and lowest (gaussian) noise's effects on the likelihood that a given pixel will be distorted. By using the weighted mean WM value of the chosen window, the primary idea behind AWMF is to inhibit spurious error detection and recover damaged pixels. Equation (2) provides the weighted mean WM value of the specified window W.

$$\mathrm{M}_{\mathrm{i,j}}^{\mathrm{mean}}(\mathrm{W}) = \begin{cases} \dfrac{\sum\limits_{\mathrm{k,l}\in \mathrm{WM}_{\mathrm{i,j}}(\mathrm{W})} \mathbb{w}_{\mathrm{i,j}} * \mathrm{dr}_{\mathrm{k,l}}}{\sum\limits_{\mathrm{k,l}\in \mathrm{WM}_{\mathrm{i,j}}(\mathrm{W})} \mathbb{w}_{\mathrm{i,j}}} & \sum\limits_{\mathrm{k,l}\in \mathrm{WM}_{\mathrm{i,j}}(\mathrm{W})} \mathbb{w}_{\mathrm{k,l}} \neq 0 \\ -1 & \text{otherwise} \end{cases} \tag{2}$$

Where, $\mathbb{w}_{i,j}$ is the weight and defined as in equation (3):

$$\mathbb{w}_{\mathrm{i,j}} = \begin{cases} 1 & \mathrm{WM}_{\mathrm{i,j}}^{\mathrm{mean}}(\mathrm{W}) < \mathbb{w}_{\mathrm{k,l}} < \mathrm{WM}_{\mathrm{i,j}}(\mathrm{W}) \\ 0 & \text{otherwise} \end{cases} \tag{3}$$

The flow of adaptive weighted mean filter is depicted in Algorithm 1.

Algorithm 1. The Methodology of Adaptive Weighted Mean Filter

1. For each pixel (i,j) in noisy image dr and restored image y, do
2. Initialize $W = 1, W_{max} = 1$
3. Compute $WM_{i,j}^{mean}(W)$
4. If $WM_{i,j}^{mean}(W) \neq -1$ then go to step (8);
5. Otherwise, $W = W + 1$.
6. If $W \leq W_{max}$, go to step (3)
7. Otherwise$re_{i,j} = M_{i,j}^{mean}(W)$ and stop. //re is the restored image
8. If $M_{i,j}^{min}(W) < dr_{i,j} < M_{i,j}^{max}(W)$, where $dr_{i,j}$is noise-free,
9. Otherwise, $dr_{i,j}$is noise candidate, $dr_{i,j} = M_{i,j}^{mean}(W)$, and stop.

In Algorithm 1, for each pixel, adaptive window size W is determined until two subsequent windows have equal maximum and lowest values, by repeatedly increasing the window sizes. If either the maximum or lowest values are same, the center pixel is then considered a noise candidate; otherwise, it is considered a noise-free pixel. Since AWMF is used, it has been shown that the detection error may be significantly

reduced, particularly for very high levels of noise. Following noise detection, the noise-free pixel is not altered; instead, the weighted mean value of the current window replaces the noise candidate. Particularly for high levels of noise, AWMF's weighted mean replaces noisy candidates better than WMF's median. The radius of the window is extended to provide a relevant weighted mean. But, in AMF, the output median takes into account their effects. The weighted mean in AWMF removes the possible impact of noisy pixels.

Most commonly available AWMF are used to remove noises, however edge blurring and low noise suppression are the two main issues with them. The filtering algorithms should keep the information accessible in order to maintain the clear and important information existing in the image. The suggested work uses a weight adaption strategy for designing the filter that is based on the Crow Optimization Algorithm. In a mean square sense, the filter weights are immediately adjusted and optimized to repair a damaged pixel. As a consequence of the suggested work, noisy pixels and their edge direction are replaced with near originals. The Peak Signal-to-Noise Ratio is one of the primary objective criteria that is taken into consideration. By introducing a novel filtering framework for noise reduction utilizing the Crow Optimization Algorithm, the suggested research study Adaptive Optimum Weighted Mean Filter (AOWMF) is created. [24].

3.2.1.1. Adaptive optimum weighted mean filter (AOWMF). The modified crow algorithm is combined with the AWMF model in the AOWMF method proposed in this section. The COA algorithm intelligently optimizes the involvement weight value $\mathbb{w}$ besides the threshold in the AWMF, and the Moore-Penrose generalized inverse matrix calculates the output $\mathbb{w}$. Then, using the noise model it creates the optimized AWMF model using COA, which use the test set to acquire the model's taxonomy outcomes for noise removed MRI images $\widehat{y}$. The precise process of the AOWMF algorithm is as follows and the flow diagram is given in Fig. 2:

1. Establish the COA and AWMF algorithms' related parameters, create a *d*-dimensional crow population at random as the noisy pixels, as well as then map the crow population using the chaos method to initialize it.
2. Initialize the population, then create and encode initial solutions at random. Each solution has $m \times (n+1)$ dimensions, with the first $m \times n$ dimension representing the input W.
3. Practice the result obtained in step 2 to work out, determine the input W, as well as the window scale starting point, then train the AWMF model on the MRI image data. Here notes a point that although the obtained solution is a vector value, which is a $m \times (n+1)$ -dimensional matrix during the pre-processing phase, which must be transformed into a vector form beforehand.
4. Compute the PSNR fitness value associated with each solution and increase the number of iterations as iter = iter +1.
5. Set the locus of a drove of N crows (pixels) in the search intergalactic at random. Set each crow's memory to zero.
6. Compute the fitness value for each solution utilizing the features as input W and calculate $dr_{i,j}$.
7. At random, a crow number j is picked. The crow i monitors the crow j and flies to the crow j's memory spot if the random number rand $j \geq P$. If the random number rand $j < P$ crow j will follow the new start given in step 9 to deceive crow i.
8. At just the beginning of iterations, the value of $\mathfrak{N}$ commences from a large number as well as is decreased as per fitness value, while at the end of iterations, wherever precise checking everywhere the paramount confined optimums is needed, the $\mathfrak{N}$ has a lesser significance. Calculate the $\mathfrak{N}$ factor as expressed in equation (4):

$$\mathfrak{N}^{\text{iter}} = \text{round}\left(\mathfrak{N}_{\max} - \frac{\mathfrak{N}_{\max} - \mathfrak{N}_{\min}}{\text{maxiter}} \times \text{iter}\right) \tag{4}$$

9. Make specially $\mathfrak{N}$ of the thoroughgoing crows in the inhabitants, excluding for the contemporary crow denoted as the i and update the point of the crow i through generating random uppermost crows from contemporary crow as the objective that denoted by j as well as generating the new position with as per equation (5):

$$\mathrm{x}^{\mathrm{i,iter}} = \begin{cases} \mathrm{x}^{\mathrm{i,iter}} + \mathrm{rand_i} \times \mathrm{fl}^{\mathrm{i,iter}} \times \left(\mathrm{Dist}^{\mathrm{i,j}}\right) & \mathrm{rand_j} \geq \mathrm{P}^{\mathrm{j,iter}} \\ \text{a random position} & \text{otherwise} \end{cases} \tag{5}$$

10. where, r_i and r_j remain the unchanging disseminated random statistics between 0 or 1, $fl^{i,iter}$ and $P^{j,iter}$ remain the crow i flight time and perception of the crow j at the repetition, with probability P *iter*, correspondingly. Through choosing a small P, the algorithm achieves an examination in the area wherever the present well-thought-of solution of the j th crow is positioned.
11. In COA, the fortitude of fl is proposed which principals to handpicked the appropriate significance of fl regarding the situations of the crows as expressed in equation (6):

$$\mathrm{fl}^{\mathrm{i,iter}} = \begin{cases} 2 & \text{if } \mathrm{Dt}^{\mathrm{i,j}} \leq \mathrm{Dt_{th}} \\ \mathrm{fl_{th}} & \text{if } \mathrm{Dt}^{\mathrm{i,j}} \leq \mathrm{Dt_{th}} \end{cases} \tag{6}$$

$$\mathrm{D}^{\mathrm{i,j}} = \mathrm{m}^{\mathrm{j,iter}} - \mathrm{x}^{\mathrm{i,iter}} \tag{7}$$

12. where, $Dt^{i,j}$ is the vector (as expressed in equation (7)) which comprises the distances stuck between the crow i and crow j which are the threshold value and $fl_{th} > 2$.
13. The data is forecasted using the contemporary crow position as the AWMF model parameter, besides the prediction outcome is rehabilitated hooked on also compared to the crow fitness function value memory position fitness function value. The memory position is changed in accordance with equation (8) if the present location is better than the memory position:

$$\mathrm{m}^{\mathrm{i,iter+1}} = \begin{cases} \mathrm{x}^{\mathrm{i,iter}} & \mathrm{f}\left(\mathrm{x}^{\mathrm{i,iter}}\right) \text{ is better than } \mathrm{f}\left(\mathrm{m}^{\mathrm{i,iter+1}}\right) \\ \mathrm{m}^{\mathrm{i,iter}} & \text{otherwise} \end{cases} \tag{8}$$

Where $x^{i,iter}$ $f(\bullet)$ stands for the objective function, it represents the *ith* crow's d-dimensional search space position vector.

14. For each crow, repeat steps 1–12, count the number of times the previous iterations' quantified values were saved, and then use them to determine the starting AWMF prediction model input weight and threshold.
15. Train the AWMF model and estimate its fitness value in order to test the novel solution created in step 13.

16. Check to see whether the AWMF algorithm's COA process has gone through all possible iterations; if so, go on to step 13; if it is not, return to step 6 to keep doing the same of the algorithm.

17. Work out the returned optimum solutions yields the optimal input $\mathbb{w}$.
18. Final denoised images obtained $\widehat{y}(i.j)$ using the AWMF model and end the process.

3.2.2. Bilateral filter

The efficiency of the bilateral filter in denoising images while keeping their edges is well recognized. The suggested work employs an iterative bilateral filter that maintains fine structures, increases denoising effectiveness, and decreases bias caused by Rician noise to

filter the noise in the magnitude magnetic resonance image [19]. The image has maintained both its visual and diagnostic qualities. Bilateral filtering works by applying standard filters to an image's range rather than just its domain, as the name implies [13]. Perhaps in a perceptually significant way, two pixels might be near to one another. Both proximity and similarity relate to the region immediately around a given object in a given domain. Traditional filtering weights pixels by distance, also known as domain filtering, promotes proximity. Comparably, range filtering averages image data using weights whose values decrease as similarity increases. Since the weights of range filters are dependent on the image intensity, they are nonlinear. Most importantly, they keep edges sharp [14]. Using a nonlinear filter known as a bilateral filter, noise may be reduced [15] without impairing crucial image elements like edges. Each neighbourhood bilateral filter kernel is made from the domain filter and range filter. A pixel's spatial distance from its surrounding area determines the domain filters weights. The radiometric distance around a pixel's neighbourhood determines how the range filter coefficients are calculated. Equation (9) represents the bilateral filter's response at pixel point x [16]:

$$\widehat{\mathrm{I}}(\mathrm{x},\mathrm{y}) = \frac{1}{\mathrm{NC}} \sum_{\mathrm{y}\in \mathrm{N}(\mathrm{x})} \mathrm{r_s}(\mathrm{x},\mathrm{y}) * \mathrm{r_r}(\mathrm{x},\mathrm{y}) * \mathrm{I}(\mathrm{y}) \tag{9}$$

$$\mathrm{NC} = \sum_{\mathrm{y}\in \mathrm{N}(\mathrm{x})} \mathrm{r_s}(\mathrm{x},\mathrm{y}) * \mathrm{r_r}(\mathrm{x},\mathrm{y}) \tag{10}$$

Where NC represent normalization factor, $N(x)$ denotes the area surrounding x in the neighbourhood, and y is the location there, r_s and r_r are, respectively, bidirectional filter domain and radiometric components, and their definitions follow equations (11) and (12):

$$\mathrm{r_s}(\mathrm{x},\mathrm{y}) = \exp\left(\frac{-|\mathrm{x}-\mathrm{y}|^2}{2\sigma_\mathrm{s}^2}\right) \tag{11}$$

$$\mathrm{r_r}(\mathrm{x},\mathrm{y}) = \exp\left(\frac{-\left|\mathrm{it_x}-\mathrm{it_y}\right|^2}{2\sigma_\mathrm{r}^2}\right) \tag{12}$$

The radiometric distance between the intensities it_x and it_y causes a drop in the weight function r_r and a decrease in the weight function r_s . Three parameters govern how smoothly two weight components decay: σ_s, σ_r and N, which governs the filter's support. The best values for σ_s and σ_r can be chosen, although there isn't much theoretical support for doing so. The ideal σ_s is shown to be somewhat noise-insensitive, whereas σ_r is practically directly proportional to the genuine noise standard deviation σ. A suitable range for σ_s, according to, should be in the following range: Let $O_1, O_2, \ldots, O_n$ be n represent the number of statistically distinct observations O from an area of constant MRI image signal intensity SI. After that, equation (13) may be used to define the joint Probability Distribution Function (PDF) of the data [21]:

$$\mathrm{PDF}(\{\mathrm{O_i}|\mathrm{SI}\}) = \prod_{\mathrm{i}=1}^{\mathrm{n}} \frac{\mathrm{M_i}}{\sigma^2} \mathrm{e}^{\frac{\mathrm{M_i^2}+\mathrm{SI^2}}{2\sigma^2}} \mathrm{I_0}\left(\frac{\mathrm{SIM_i}}{\sigma^2}\right) \tag{13}$$

Given the observed data and an interest model, the unknown parameters in the PDF may be computed by maximizing the related likelihood function LF(SI) or, alternatively, ln LF(SI), as indicated in equation (14).

$$\ln \mathrm{LF}(\mathrm{SI}) = \sum\nolimits_{\mathrm{i}=1}^{\mathrm{n}} \ln\left(\frac{\mathrm{M_i}}{\sigma^2}\right) - \sum\nolimits_{\mathrm{i}=1}^{\mathrm{n}} \frac{\mathrm{M_i^2}+\mathrm{SI^2}}{2\sigma^2} + \sum\nolimits_{\mathrm{i}=1}^{\mathrm{n}} \ln\left(\frac{\mathrm{SI}*\mathrm{M_i}}{\sigma^2}\right) \tag{14}$$

The *ML* the global maximum of an estimate is then discovered ln LF w.r.t SI and σ^2 as per equation (15):

$$\left\{\widehat{\mathrm{SI}}_{\mathrm{M*LF}}, \widehat{\sigma}^2_{\mathrm{M*LF}}\right\} = \underset{\mathrm{SI},\sigma^2}{\mathrm{argmax}}\{\ln \mathrm{LF}\} \tag{15}$$

In order to estimate the signal and noise variance, this approach takes the underlying signal in the immediate vicinity to be constant. The mode of all MLF estimated local noise levels in equation may be used as a reliable estimator for the noise variance (16) if this assumption holds true for the majority of local neighbourhoods:

$$\widehat{\sigma}^2 = \mathrm{mode}\left\{\widehat{\sigma}^2_{\mathrm{MLF(i)}}\right\} \tag{16}$$

where $\widehat{\sigma}^2_{M*LF}$ utilizing a small local neighbourhood, is the image's local noise variance estimate at pixel i. Being independent of the Rayleigh dispersed background area for noise estimation is a benefit of this technique. It should be noted that the MLE must be determined numerically using optimization techniques after the equation's parameters cannot be determined through a closed form solution (17). In this procedure, bias is reduced before using the bilateral filter again [17]. Bias may be reduced by deleting the Rice distribution's second moment $2\sigma^2$ based on the squared image. Let $\widehat{I}_i$ be the denoised image after i iterations, and the bias in the image is rectified as in equation (17).

$$\widehat{\mathrm{I}}_\mathrm{i} = \sqrt{\max\left(\mathrm{I_i^2} - 2\widehat{\sigma}^2, 0\right)} \tag{17}$$

The noise level is now reduced after each iteration of the bilateral filter, and this requires re-estimating the noise level each time. After each repetition, the approach described in equation (18) is applied to estimate noise.

4. Experimental results and discussion

The section presents the findings from a comparative examination of several approaches and the recommended framework. AMRG cardiac MRI Atlas images and the SCMR consensus dataset were used to get the experimental results. The objective function of the suggested AOWMF using BF methods has been the peak signal to noise ratio (PSNR). Gaussian, Salt-Pepper, Rician, and Speckle noise is applied to the preferred images from the dataset at the start of the experiment. Using the suggested framework as shown in the technique section, this contaminated image with various noises is denoised. To increase performance, the proposed model's results are tested using cardiac MRI data, and its results are compared to those of current techniques such as adaptive weighted mean and homomorphic filtering and nonlocal maximum likelihood (NLM). (AWMF-HF). PSNR, NAE, MSE, and structural SSIM have all been used to determine the quantitative or measurably effective nature of the suggested denoising approach [18].

4.1. Performance metrics

4.1.1. Peak signal to noise ratio (PSNR)

The PSNR is a popular metric that is used widely for evaluating the quality of the recovered image I_{res}. The parameter's definition is that it measures how much noise there is in a denoised medical image in relation to its peak signal power I_{den}. In accordance with equation (18), a greater PSNR value implies a scheme's improved capacity for denoised:

$$\mathrm{PSNR} = \log_{10}\frac{\mathrm{I_{max}^2}}{\mathrm{MSE}} \tag{18}$$

4.1.2. Normalized absolute error (NAE)

The error value calculated from the intensity differences is shown as the normalized absolute error. According to equation (19), a number closer to zero implies less inaccuracy in the reconstructed image.

$$\mathrm{NAE} = \frac{\sum_{\mathrm{m}=0}^{\mathrm{M}-1}\sum_{\mathrm{n}=0}^{\mathrm{N}-1}\left|\mathrm{I_{ref}}(\mathrm{m},\mathrm{n}) - \mathrm{I_{den}}(\mathrm{m},\mathrm{n})\right|}{\sum_{\mathrm{m}=0}^{\mathrm{M}-1}\sum_{\mathrm{n}=0}^{\mathrm{N}-1}\left|\mathrm{I_{ref}}(\mathrm{m},\mathrm{n})\right|} \tag{19}$$

Table 1
The numerical results of NLM, AWMF-HF and AWMF-BF

Methods	PSNR (dB)	NAE (%)	MSE (%)	SSIM
NLM	35	0.72	0.48	0.95
AWMF-HF	45	0.67	0.42	0.97
AOWMF-BF	65	0.18	0.24	0.98

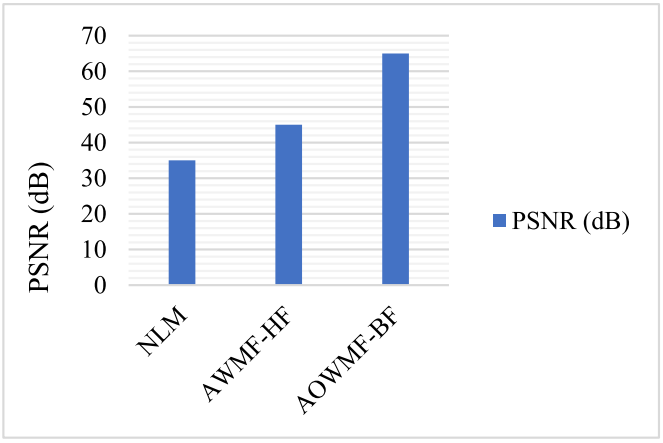

Fig. 3. Comparative PSNR analysis of different methods.

4.1.3. Mean square error (MSE)

In order to assess distortion, mean square error is often utilized. The parameter calculates the square root of the average error. The expression for this non-negative parameter is equation (20), where values nearer to zero are preferable:

$$\mathrm{MSE} = \frac{1}{MN}\sum_{m=0}^{M-1}\sum_{n=0}^{N-1}\left[I_{ref}(m,n) - I_{den}(m,n)\right]^2 \tag{20}$$

4.1.4. Structural similarity index measurement (SSIM)

Index of Structural Similarity to determine how closely the reference image I_{ref} and the denoised image resemble each other, measurement is calculated. Its value ought to fall between [0, 1]. Equation (21)'s representation of the parameter calculation shows that a higher value represents a better restored image:

$$\mathrm{SSIM} = \frac{\left(2\mu_{I_{ref}}\mu_{I_{den}} + v_1\right)\left(2\sigma_{I_{ref}}\mu_{I_{den}} + v_2\right)}{\left(\mu^2_{I_{ref}} + \mu^2_{I_{den}} + v_1\right)\left(\mu^2_{I_{ref}} + \mu^2_{I_{den}} + v_2\right)} \tag{21}$$

where, μ consists of the image's average and σ if the image variations. Two variables are used to stabilize the weak denominator in this v_1 and v_2.

The performance of AOWMF and BF based denoising approach is found to be effective as compared with Non-Local Maximum Likelihood (NLM) and Adaptive Weighted Mean and Homomorphic Filtering (AWMF-HF) [20]. The best values of MSE, NAE, SSIM, and PSNR in Table 1 show that this is the case. This was accomplished by using nonlocal pixel similarity to take use of the redundant information in the image and COA-based weight value optimization of AWMF. This demonstrates superior denoising while maintaining image details. Moreover, it is discovered that using AOWMF-based approaches improves all of the parameters in the evaluation indices. Table 1 displays the numerical findings, which demonstrate how effective the method was at maintaining structural information in medical images. In contrast to previous approaches, its non-iterative process makes it computationally efficient. A better registration of image details with less inaccuracy is shown by the best NAE scores.

The comparative study of PSNR as acquired using various methodologies is shown in Fig. 3 along with the suggested model. As compared to other approaches, the PSNR value achieved by the suggested framework is determined to be superior. The suggested method's PSNR value is 65 dB, which is greater than that of the NLM and AWMF-HF methods. According to these results, the AOWMF and BF are the most effective in reducing noise and improving the visual clarity of medical images.

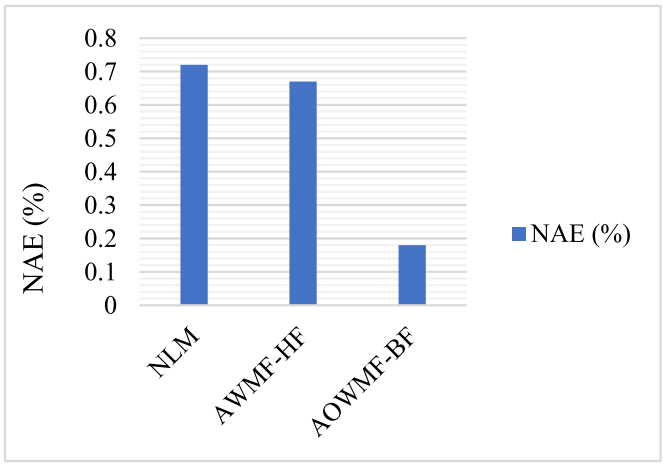

Fig. 4. Comparative NAE analysis of different methods.

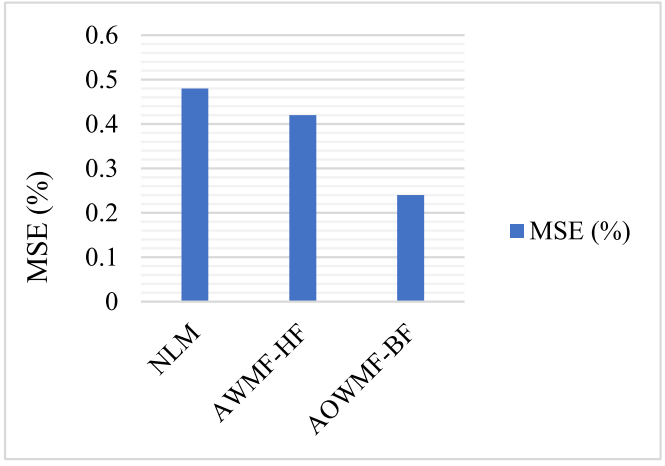

Fig. 5. Comparative MSE analysis of different methods.

Fig. 4 illustrates the comparative analysis of NAE as obtained using different techniques with the proposed model. The NAE value obtained using the proposed framework is found to be better as compared to the other methods. The NAE value of proposed method is 0.18%, which is lower than the same as obtained using NLM and AWMF-HF method. This may be due to the nonlocal COA based AWMF where the weight values are chosen optimally for the images by automatic estimation of window and denoised image.

The comparison of various strategies with the suggested model using MSE is shown in Fig. 5. As compared to other techniques, the MSE value achieved by the suggested framework is determined to be superior. The MSE value obtained using the proposed method is 0.24%, which is lower than the same as obtained using NLM and AWMF-HF method. Better registration of the image details is shown by the MSE values. The findings further show that Speckle and Gaussian noise in MR images may be effectively removed using AOWMF-based approaches. Since the performances of the previous approaches are constrained by their computational complexity, the findings of existing methods achieved significant MSE.

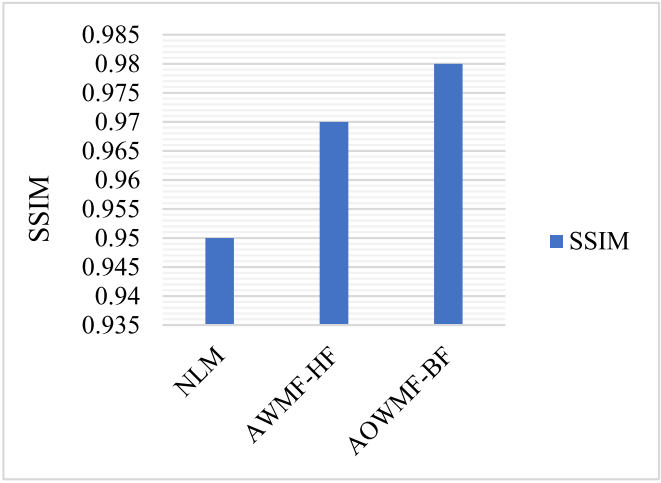

Fig. 6. Comparative SSIM analysis of different methods.

Fig. 6 shows an examination of the SSIM produced using various methodologies and the suggested model in comparison. In comparison to other techniques, the SSIM value achieved by the suggested framework is determined to be superior. The SSIM value of the proposed method is observed as 0.98, which is higher than the same as obtained using NLM and AWMF-HF method. The AOWMF and BF model was built to find the best results of denoising of MRI images. The bilateral filter enhances the SSIM findings by removing the majority of the texture, noise, and small details while maintaining the large, sharp edges without blurring. The figure demonstrates that the hybridization of COA and AWMF is the method that achieves the greatest results in terms of denoising while still maintaining structural features. Although BF eliminates the majority of the texture, noise, and tiny details, it keeps the broad, sharp edges without blurring edges, but the optimal value of AWMF using this technique shows superior registration of the image features.

5. Conclusion and future work

In this work an AOWMF and BF algorithm for cardiac MRI image denoising is proposed and tested on noisy images. Low contrast in MRI images is the fundamental flaw, making it difficult to diagnose disorders accurately. Many denoising methods have been suggested by researchers. The bilateral filer (BF) is the most popular algorithm for edge preserving denoising used for Rician images. The high-level Speckle and Gaussian type of noises can be eliminated by using AOWMF algorithm. Using COA, which reduces the mean square error rate, the weights in the proposed AOWMF have been optimized. On the basis of performance parameters including PSNR, NAE, MSE, and SSIM, it has been noted from the findings that the AOWMF and BF outperform the currently used approaches. The performance of the remaining various postprocessing techniques used on the MR data, such as segmentation and registration, may be adversely affected by frequent denoising since it may cause the loss of certain features and edges in images that are highly important and very vital. It may be difficult to prevent over-contrast enhancement, reduce noise in uniform areas, and maintain the fine details of the original picture while simultaneously lowering noise in uniform regions. To get around these limitations, contrast enhancement based on other effective method to be focused in future.

Declaration of competing interest

The authors declare that they have no known competing financial interests or personal relationships that could have appeared to influence the work reported in this paper.

Data availability

https://www.cardiacatlas.org/scmr-consensus-contours/

References

[1] A.S. Fahmy, Background noise removal in cardiac magnetic resonance images using Bayes classifier, in: 2008 30th Annual International Conference of the IEEE Engineering in Medicine and Biology Society, IEEE, 2008, August, pp. 3393–3396.
[2] V. Shlykov, V. Kotovskyi, N. Višniakov, A. Šešok, Model for elimination of mixed noise from MRI heart images, Appl. Sci. 10 (14) (2020) 4747.
[3] J. Mohan, V. Krishnaveni, Y. Guo, A survey on the magnetic resonance image denoising methods, Biomed. Signal Process Control 9 (2014) 56–69.
[4] N. Kumar, M. Nachamai, Noise removal and filtering techniques used in medical images, Orient. J. Comput. Sci. Technol. 10 (1) (2017).
[5] A. Ouahabi, May). A review of wavelet denoising in medical imaging, in: 2013 8th International Workshop on Systems, Signal Processing and Their Applications (WoSSPA), IEEE, 2013, pp. 19–26.
[6] M. Bouhrara, M.C. Maring, R.G. Spencer, A simple and fast adaptive nonlocal multispectral filtering algorithm for efficient noise reduction in magnetic resonance imaging, Magn. Reson. Imag. 55 (2019) 133–139.
[7] A. Weber, J. Weizenecker, U. Heinen, M. Heidenreich, T.M. Buzug, Reconstruction enhancement by denoising the magnetic particle imaging system matrix using frequency domain filter, IEEE Trans. Magn. 51 (2) (2015) 1–5.
[8] Y.L. Zhang, W.Y. Liu, I.E. Magnin, Y.M. Zhu, Feature-preserving smoothing of diffusion weighted images using nonstationarity adaptive filtering, IEEE (Inst. Electr. Electron. Eng.) Trans. Biomed. Eng. 60 (6) (2013) 1693–1701.
[9] B. Stimpel, C. Syben, F. Schirrmacher, P. Hoelter, A. Dörfler, A. Maier, Multi-modal deep guided filtering for comprehensible medical image processing, IEEE Trans. Med. Imag. 39 (5) (2019) 1703–1711.
[10] K. Murugan, V.P. Arunachalam, S. Karthik, Hybrid filtering approach for retrieval of MRI image, J. Med. Syst. 43 (1) (2019) 1–8.
[11] J. Yang, J. Fan, D. Ai, S. Zhou, S. Tang, Y. Wang, Brain MR image denoising for Rician noise using pre-smooth non-local means filter, Biomed. Eng. Online 14 (1) (2015) 1–20.
[12] SCMR Consensus Data – Cardiac Atlas Project(Accessed on 4.January.2022).
[13] S. Routray, P.P. Malla, S.K. Sharma, S.K. Panda, G. Palai, A new image denoising framework using bilateral filtering based non-subsampled shearlet transform, Optik 216 (2020), 164903.
[14] F.A. Jassim, Image Denoising Using Interquartile Range Filter with Local Averaging, 2013 *arXiv preprint arXiv:1302.1007*.
[15] D. Bhonsle, V. Chandra, G.R. Sinha, Medical image denoising using bilateral filter, Int. J. Image Graph. Signal Process. 4 (6) (2012) 36.
[16] J.W. Han, J.H. Kim, S.H. Cheon, J.O. Kim, S.J. Ko, A novel image interpolation method using the bilateral filter, IEEE Trans. Consum. Electron. 56 (1) (2010) 175–181.
[17] P.D. Patil, A.D. Kumbhar, Bilateral filter for image denoising, in: 2015 International Conference on Green Computing and Internet of Things (ICGCIoT), IEEE, 2015, October, pp. 299–302.
[18] S. Saladi, N. Amutha Prabha, Analysis of denoising filters on MRI brain images, Int. J. Imag. Syst. Technol. 27 (3) (2017) 201–208.
[19] R. Riji, J. Rajan, J. Sijbers, M.S. Nair, Iterative bilateral filter for Rician noise reduction in MR images, Signal, image and video processing 9 (7) (2015) 1543–1548.
[20] P. Yugander, et al., MR image enhancement using adaptive weighted mean filtering and homomorphic filtering, Proc. Comput. Sci. 167 (2019) (2020) 677–685, https://doi.org/10.1016/j.procs.2020.03.334. Elsevier B.V.
[21] A. Askarzadeh, A novel metaheuristic method for solving constrained engineering optimization problems: crow search algorithm, Comput. Struct. 169 (2016) 1–12.